Cum Laude Poster Award, Best Student Paper Runner-Up

Multi-modality Fusion of CT, 3D Ultrasound, and Tracked Strain Images for Breast Irradiation Planning

Pezhman Foroughi[a], Csaba Csoma[a], Hassan Rivaz[a], Gabor Fichtinger[a,b], Richard Zellars[c], Gregory Hager[a], and Emad Boctor[a,c]

[a]Department of Computer Science, Johns Hopkins University, Baltimore, USA;
[b]School of Computing, Queen's University, Kingston, Canada;
[c]Department of Radiology, Johns Hopkins University, Baltimore, USA

ABSTRACT

Breast irradiation significantly reduces the risk of recurrence of cancer. There is growing evidence suggesting that irradiation of only the involved area of the breast, partial breast irradiation (PBI), is as effective as whole breast irradiation. Benefits of PBI include shortened treatment time, and perhaps fewer side effects as less tissue is treated. However, these benefits cannot be realized without precise and accurate localization of the lumpectomy cavity. Several studies have shown that accurate delineation of the cavity in CT scans is very challenging and the delineated volumes differ dramatically over time and among users.

In this paper, we propose utilizing 3D ultrasound (3D-US) and *tracked* strain images as complementary modalities to reduce uncertainties associated with current CT planning workflow. We present the early version of an integrated system that fuses 3D-US and real-time strain images. For the first time, we employ tracking information to reduce the noise in calculation of strain image by choosing the properly compressed frames and to position the strain image within the ultrasound volume. Using this system, we provide the tools to retrieve additional information from 3D-US and strain image alongside the CT scan. We have preliminarily evaluated our proposed system in a step-by-step fashion using a breast phantom and clinical experiments.

Keywords: Tracked Strain, 3D Ultrasound, Breast Cancer, Partial Breast Irradiation

1. INTRODUCTION

Radiation therapy is an integral part of the management of early stage breast cancer. Although breast conserving therapy (BCT) provides excellent local control and equivalent survival to modified radical mastectomy in appropriately selected patients, this achievement is not without physical and social costs. Specifically the physical cost of radiation includes but is not limited to skin, lung and heart damage, rib fracture, pain, and poor cosmesis. Radiation in BCT is typically given daily over 5-7 weeks, negatively impacting quality of life.

To allow greater freedom of choice, altered breast-conserving therapies, such as lumpectomy alone with wide margins and cryotherapy have been developed. The goal of these therapies was to provide the same local control and survival as traditional BCT, but at a much lower social and physical cost. Currently, the most promising non-standard therapy is partial breast irradiation (PBI). The goal of PBI is to treat the lumpectomy with a margin while minimizing dose to the surrounding breast tissue and vital organs. External beam radiation therapy (EBRT) is probably the most appealing PBI technique, especially for community radiation centers, due to its apparent simplicity, predictability, and applicability to other organ systems.[1]

Precise localization of the lumpectomy bed is mandatory for PBI. In contemporary practice, imprecise target localization often results in poor local control which leads to unnecessary and possibly severe skin toxicity.[2]

Further author information: (Send correspondence to P. Foroughi)
P. Foroughi, G. Hager: E-mail: (pezhman,hager)@cs.jhu.edu
C. Csoma, H. Rivaz: E-mail: (csoma,rivaz)@jhu.edu
G. Fichtinger: E-mail: gabor@cs.queensu.ca
R. Zellars, E. Boctor: E-mail: (zellari,eboctor1)@jhmi.edu

Medical Imaging 2009: Ultrasonic Imaging and Signal Processing, edited by Stephen A. McAleavey, Jan D'hooge
Proc. of SPIE Vol. 7265, 72651B · © 2009 SPIE · CCC code: 1605-7422/09/$18 · doi: 10.1117/12.812878

Further progress of PBI critically depends on the availability of a method for a non-invasive and non-toxic real-time 3D visualization of the targeted volume.

Techniques based on external landmarks or combination of CT scan and surgical clips[2] are far from being satisfactory. The CT scan can be insensitive to subtle changes in breast tissue and the surgical clips delineate only part of the tumor bed, making a true 3D map of the tumor cavity often unattainable. The volumetric accuracy of such discrete markers is well studied and known to be extremely sensitive to the number and relative pose of the markers,[3] thereby rendering this approach inadequate for inferring the shape, volume, and location of complex tumor beds. Furthermore, the small titanium clips are not visible on conventional and electronic portal imaging. While kV fluoroscopy localization of the clips would be useful, such units are very rarely available today and also raise several practical problems. Flat panel cone beam computed tomography[4] has been investigated, but this approach has limitations in soft tissue contrast,[5,6] requires specialized hardware added on the therapy machine.[7] Breast targets often move significantly after a pre-treatment setup, but repeated cone beam imaging sessions would exposes the patient to excessive radiation dose. PBI also requires peculiar beam directions in which the on-board kV sources and detectors tend to interfere with the couch.

As a result, CT alone is currently used in many departments for delineating the surgical bed. In a recent study,[8] CT images of 33 patients were obtained. Four radiation oncologists were asked to delineate the surgical beds. 4 cases had no visible cavity and were declined by the physicians. In the remaining 29 cases, the average percent overlap between the delineated volumes ranged from 57% to 87% for images with low to high visible cavities. The shift of the center of mass of the delineated volume was from 1.5 mm to 6.9 mm for images with high to low visible cavities. The work concluded that even among radiation oncologists who specialize in breast radiotherapy, there can be substantial differences in delineation of the lumpectomy bed.

Another recent work[9] showed that the definition of the lumpectomy bed based on CT images requires further investigation. The delineated cavity not only varies between observers, but also changes during the course of treatment. The work concludes that the variations in the volume of the lumpectomy bed during a course of radiotherapy are significant in relation to current clinical inter-observer variations. This is an important finding to take into account when introducing CT based planning, especially when applying integrated radiotherapy.

Toward non-invasive and non-toxic target localization, 2D ultrasound based localization has also been tried, primarily on prostate.[10,11] Typically, the ultrasound probe is tracked and spatially registered with the coordinate frame of the of the linear accelerator's (linac) gantry, so the pixels of the B-mode images are known in the coordinate frame of the linac. Thus if one localizes the target anatomy in the B-mode images, then the position of the target is automatically known with respect to the linac's isocenter, so the patient can be re-positioned so that the target lines up under the isocenter as planned.

In this paper, we have proposed the combination of 3D-US and strain images with CT to improve the delineation of lumpectomy bed in breast cancer patients. For this goal, we have developed a system that captures the ultrasound data, constructs the 3D-US, and visualizes the 3D volume and tracked ultrasound or strain planes in real-time. The additional data then assists the surgeon for delineation of the lumpectomy bed. To the best of our knowledge, we are the first to track the strain images not only to locate the strain image within the 3D-US, but also to improve the calculation of elasticity by choosing the properly compressed frames. We have carried out breast phantom and patient experiments to evaluate our system.

2. METHODS

The PBI procedure commonly involves the following steps. Initially, the breast cancer patients undergo lumpectomy in which the cancerous lump is removed. After about four weeks, the CT scan of the breasts is acquired for planning the irradiation. Next, the surgeon manually delineates the lumpectomy bed in the CT images. The segmented area specifies the region of the breast which will be treated during EBRT, where external radiation beams are focused on the lumpectomy bed. The therapy aims to maximize the dose to the involved portion of the breast while minimizing it to the surrounding tissue and vital organs.

Our approach introduces minimal divergence from the original workflow of PBI treatment. We have an approved institutional review board (IRB) protocol to obtain B-mode and strain images from patients who undergo lumpectomy. We acquire the ultrasound data when the patients return for the CT scan four weeks after

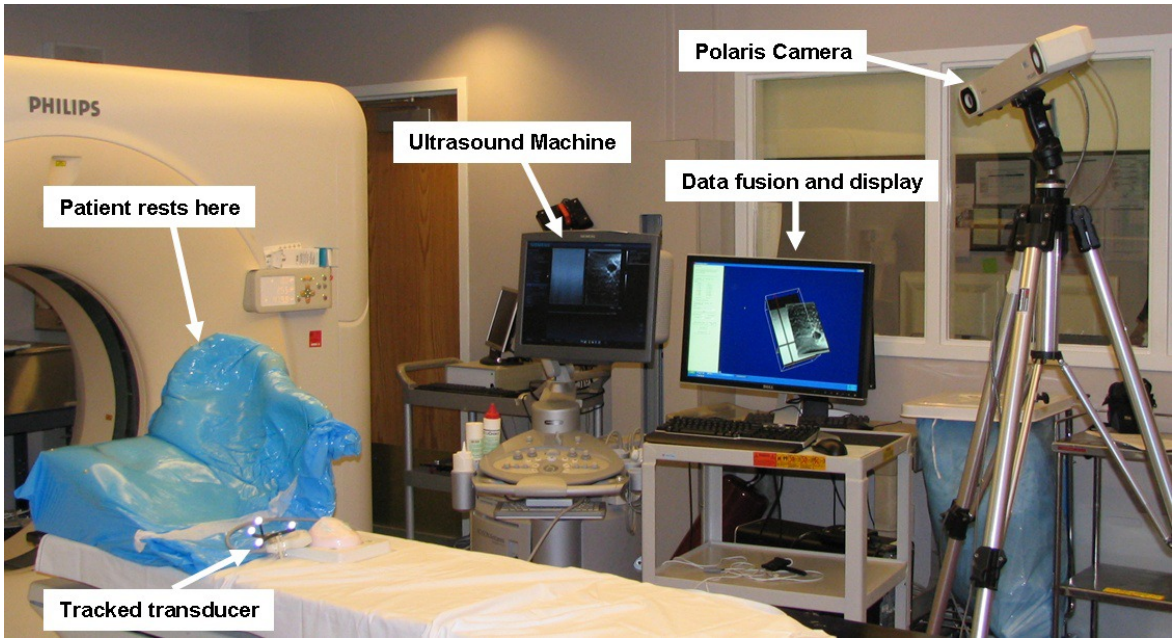

Figure 1. The components of the planning system.

the surgery. The data includes tracked B-mode images scanned over the lumpectomy bed, tracked real-time strain images, and RF dara synchronized with the tracking information for off-line processing. We have devised a data collection system for this purpose shown in Figure 1.

2.1 Workflow

Before acquiring the CT scan, four CT-compatible fiducials are placed around the scar of the surgery on patient's breast. These fiducials are additional to the ones that are commonly placed on patient's chest and the resting foam bed. The foam bed, shown in Figure 1 maintains the configuration of patient's body during the treatment. The extra fiducials are used to locally align the CT and ultrasound data, and the regular ones are used for targeting at the time of irradiation.

The patient remains in the same resting position after the CT scan. As the first step, the sonographer digitizes the location of the fiducials with a calibrated stylus by simply touching each of the four fiducials with the stylus in a certain order prescribed in our protocol.

Afterwards, the sonographer sweeps the ultrasound transducer over the lumpectomy bed collecting at least 500 B-mode images. Then within a few seconds, the program constructs the ultrasound volume from the collected images. Next, the sonograhper obtains individual tracked strain images from the areas of interest by gently moving the ultrasound transducer up and down. The visualization program demonstrates the flying strain image over the ultrasound volume (Figure 2). Depending on each case, we acquire a minimum of 200 strain images. Lastly, we record sequences of RF signals as the sonographer compresses and decompresses the tissue. The RF data synchronized with the tracking information facilitates more elaborate strain imaging techniques.

When the surgeon delineates the lumpectomy bed in CT images in the planning stage, the additional data will be available for him/her to aid the delineation. The B-mode, 3D-US, and CT volumes are resliced based on the strain images. These images as well as the corresponding slices in ultrasound and CT volumes will be presented to the surgeon. The visualization software shows the relative positions of the slices across different modalities. The surgeon performs the delineation with the same software used in original PBI workflow.

2.2 Integrated Software

We have developed a software application that has enabled fast and smooth data collection and visualization. The application interfaces with the ultrasound machine and the tracker (optical or magnetic), synchronizes, records,

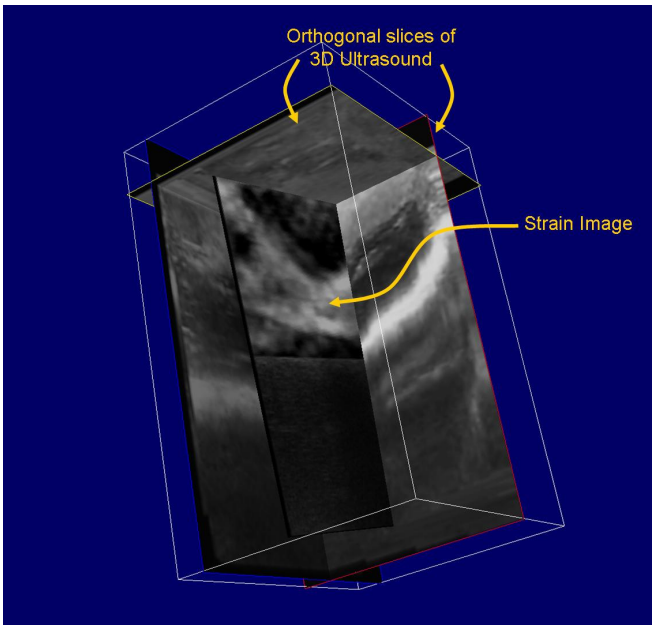

Figure 2. A snapshot of visualized 3D-US volume and the overlaid strain image.

and visualizes the data. It is implemented in C++ with a multi-threaded scheme for better performance. We have also developed a simple and intuitive graphical user interface (GUI).

B-mode images and transducer locations are continuously stored in two circular buffers in separate threads with the highest rate possible. A time-stamp with microsecond accuracy is also recorded along with the captured data. A constant delay calculated off-line is applied to synchronize the stream of data. Acquisition of B-mode images is fast, and the region of interest can be scanned within a few seconds. The maximum rate of storing data is bounded with the minimum of frame rate of the B-mode images and the tracker. However, the user can set the rate of data storage to a lower rate through the GUI if needed. Due to the high data rate and large frame sizes captured per second (typically 10 to 30 frames per second), immediate saving to the hard drive may result in unexpected delays or loss of frames. Therefore, the data is first stored in the random access memory (RAM) of the computer and stored in hard disk only when the data collection is stopped.

Once the B-mode scan is acquired, the program constructs a 3D-US volume. The volume is presented as three orthogonal slices that can be freely translated and rotated in space as shown in Figure 2. VTK (Kiteware Inc.) is mainly used for the visualization and reslicing tasks. The real-time strain images are captured in the same manner except that the strain plane is overlaid on 3D-US. In addition, the program can sends commands to ultrasound machine for capturing sequences of RF data. When the ultrasound machine receives the command, captures and saves one sequence of RF frames, while our program records the tracking information.

We have also developed an off-line program for presenting the collected data to the surgeon for delineation. This program aligns and reslices the CT volume and the ultrasound volume based on the position of strain image. The three slices (CT, B-mode, and strain) are then shown side by side.

2.3 Tracked Strain Imaging

For freehand data collection, the quality of strain images becomes extremely sensitive to the level of expertise of the user. The best result is achieved when the user compresses and decompresses the tissue uniformly in the axial direction. Any rotational or out-of-plane motion can render the collected frames unusable. Sophisticated algorithms can partially address the problem by compensating for in-plane motions and applying smoothness constraints. However, they demand large computational resources and more processing time. Moreover, they remain vulnerable to out-of-plane and large in-plane motions due to speckle decorrelation. The dependency of the quality of this imaging technique to the physician's skill has limited widespread application of strain imaging.

With typical ultrasound settings for strain imaging, we can easily capture about 30 RF frames per second. Considering the large size of each RF frame (a typical frame size would be 1800×360), only simple and efficient strain algorithms can process the frames in real-time. As a result, a large percentage of the images in the strain sequence will be noisy and unusable. The physicians generally prefer a stable and high quality strain image, which implies that the same frame rate is not necessary for strain display. The frame rate can be reduced by simply dropping the frames. Nonetheless, omitting the frames blindly does not guarantee high quality strain images, and the dependency problem will remain intact.

Here, the main idea is to select the best pairs of RF frames from the pool of images by incorporating the information from an external tracker. This is especially suitable for our system since the external tracking comes with no extra cost as a part of the system. The same idea can be applied to any other application where the ultrasound probe is tracked (e.g. ultrasound-guided navigation systems). For selection of the best pair, we take into account the properties of the motion estimation algorithm used for calculation of strain images. Automatic selection of RF pairs allows for sophisticated and computationally intensive algorithms, and at the same time, it reduces the dependency to the user.

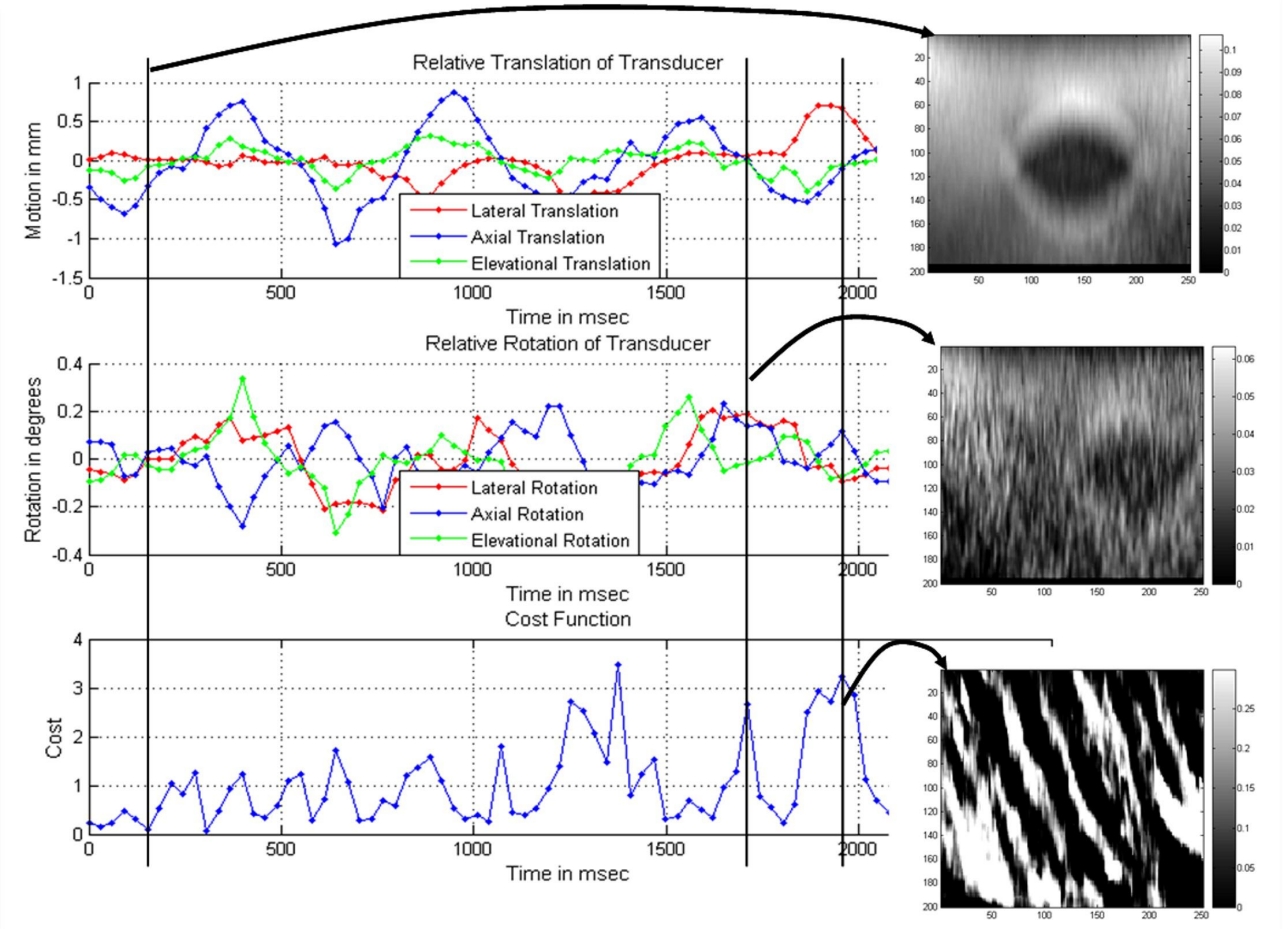

Figure 3. The proper RF pairs can be automatically selected based on the tracking information. The top image is computed using a pair of images in which the relative lateral and elevational translations and the relative rotational motions are close to zero. This is reflected in the lower value of the cost function. In the middle image, the relative axial translation is close to zero resulting in the poor contrast in strain image. In the bottom image, large lateral motion has caused the motion estimation to fail. The standard 1D NCC is used to calculate the strain images.

To this end, we have defined a heuristic cost function, $C(I_1, I_2)$, that evaluates the relative motion of the image frames I_1 and I_2 in RF sequence:

$$C(I_1, I_2) = \left[\frac{(\|T_{axl}\| - t_{opt})^2}{\|T_{axl}\| + c} + k_1 T_{ltr}^2 + k_2 T_{elv}^2 \right] + k_\alpha (\frac{1}{2} D)^2 (\alpha_{axl}^2 + \alpha_{ltr}^2 + \alpha_{elv}^2), \quad (1)$$

where T_{axl}, T_{ltr}, and T_{elv} represent the relative translation in axial, lateral, and elevational directions respectively. For a transducer facing down, these motions corresponds to "up and down", "left and right", and "out-of-plane" motions. α_{axl}, α_{ltr}, and α_{elv} symbolize the Euler angles about their corresponding axis in the same order, and D shows the depth of the image. It should be noted that I_1 and I_2 are not necessarily consecutive frames. The cost function can be evaluated for any pair of frames within a reasonable time distance.

Parameters, t_{opt}, c, k_1, k_2, and k_α, are set depending on the characteristics of the strain imaging algorithm. t_{opt} is the optimum compression(decompression) for the algorithms to construct strain image. The contrast of strain image degrades when the compression is too small. c, a positive number, governs the cost for small compressions. Considering the sensitivity of the algorithm to the unwanted motions, the parameters k_1, k_2, and, k_α are selected. As an example, for 1D motion estimation, k_1 and k_2 should be both set to high values, whereas for 2D algorithms, k_1 should be smaller than k_2. Figure 3 shows the cost function for transducer motion in an RF sequence. For a small rotation, α, the average displacement is approximately $\frac{1}{2} D\alpha$. Multiplying the factor $(\frac{1}{2} D)^2$ to the rotation values loosely converts the rotations to average displacements. This factor eliminates the dependency of k_α to the depth of the image. This cost function is minimized in order to find the best pair of images for calculation of the strain image.

2.4 System Specifications

The ultrasound data was acquired using a SONOLINE Antares^{TM} ultrasound system (Siemens Medical Solutions USA, Inc.) with a high frequency ultrasound transducer (VF10-5). Access to RF data was obtained through the Axius Direct^{TM} Ultrasound Research Interface provided by Siemens. Two different tracker systems were adopted: the "Polaris" optical tracker (Northern Digital Inc., Waterloo, Canada) with passive markers and the "Ascension" magnetic tracker (Ascension Technology Corporation, Burlington, VT) with mid-range transmitter and 6 degrees of freedom sensors. The ultrasound transducer was calibrated using the standard cross-wire calibration[12] in both cases. The B-mode ultrasound images were captured with a "WinTV" capture card (Hauppauge Computer Works, Hauppauge, NY) via s-video connection.

3. EXPERIMENTS AND RESULTS

We carried out three sets of experiments. First, we obtained B-mode and strain data from two breast cancer patients without tracking (Section 3.1). The purpose was to initially determine if the inclusion of B-mode and strain imaging can reveal any additional information that might be useful for the delineation of lumpectomy bed. Second, we evaluated our newly developed system and applications on a breast phantom. These experiments assured the reliability, speed, and functionality of the whole system for real patient experiment (Section 3.2). Finally, we examined the complete system with real patients and tracked B-mode and strain images (Section 3.3). The full patient experiments are still ongoing on regular bases of 2 to 4 patients per month.

3.1 Untracked patient experiments

We initially assessed the addition of B-mode and strain images using two patient experiments. We captured RF and B-mode data besides CT from the breast cancer patients (without tracking). We employed the elasticity algorithm developed in[13] to generate high quality strain images. Figure 4 shows snapshots of results for the first two patients. The lumpectomy bed is harder than normal breast tissue (dark in the strain image) and is hypo-echoic (dark in B-mode image). In patient 1 and 2, the red curves enclose the areas that satisfy both conditions. In patient 1, the green curve and arrows point to the area that are not hard in the strain image but are hypo-echoic in B-mode image. These preliminary results are very promising and indicate that B-mode image alone is not enough for visualizing the lumpectomy bed. However, B-mode and strain image together might provide enough information to guide PBI. Also, since ductal tissues looks almost the same as the lumpectomy bed in CT, there can be substantial differences in delineation of the surgical bed among specialists), B-mode and strain images can be added to CT to help the delineation.

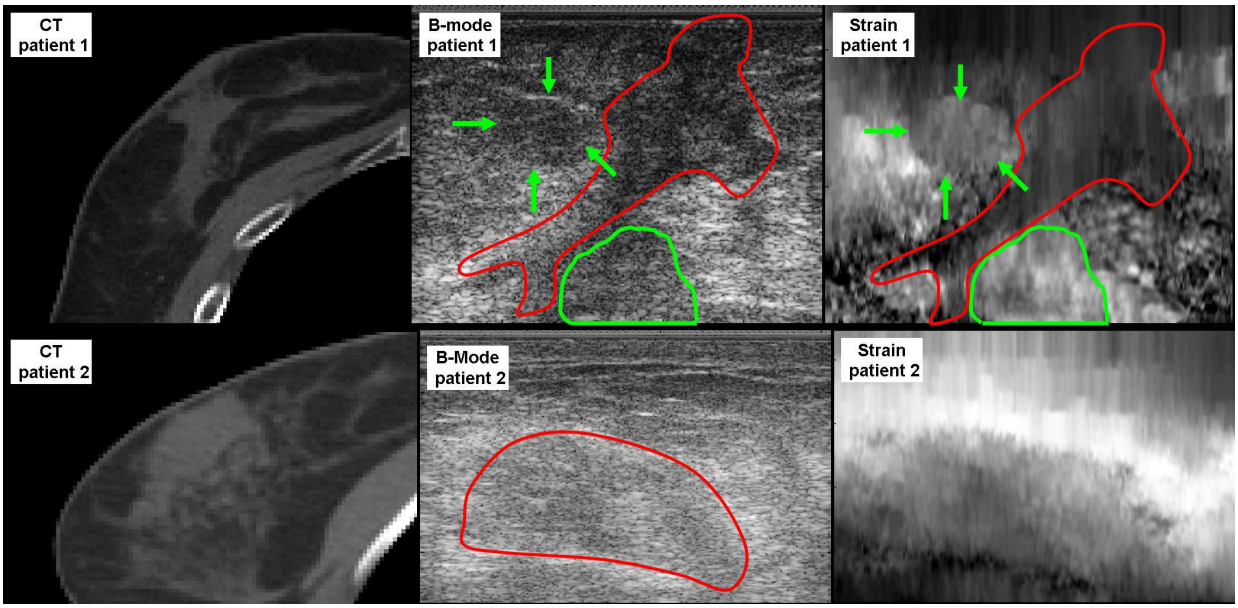

Figure 4. CT, B-mode and strain images from the first two patients.

3.2 Breast phantom experiment

To test and synchronize our system prior to the real patient experiments, a breast phantom with multiple artificial lesions inside was scanned. This phantom mimics the properties of human breast. The acoustic properties of the lesions are similar to the surrounding material, but the mechanical properties are different (the lesions are several times harder). Therefore, the lesions are easily detectable with strain images, but not visible in the B-mode image. The segmentation of the lesions matched the results of CT segmentation.

Synchronization between the RF frames and the tracking data is vital for the proposed method of selecting the best pair of images for strain computation. In order to calculate the synchronization delay, we rapidly moved the stationary transducer away from the phantom that was being imaged. The result was a sudden shift in the tracking data as well as a sudden loss of the signal energy in RF. We recovered the delay by matching these two events. Repetition of this experiment did not affect the computed value for delay noticeably. Finally, we calculated the frame transformations at the arrival time of each frame by separately interpolating the translations and rotations. We employed "spline" interpolation for the translations and "spherical linear interpolation" (Slerp)[14] for the rotations. With this setup, we were able to find the pairs of RF data that were suitable for strain imaging as shown in Figure 3.

3.3 Tracked patient experiments

In this stage, we collected tracked data from 7 breast cancer patients. We have an active IRB to collect data from 20 patients for this phase of the study. System setup requires about 15 minutes, which is completed before the arrival of the patient. For the convenience of the sonographer, we have chosen two different arrangements for the location of ultrasound machine, the computer, and the tracker depending on whether the left or the right breast is being treated. The overall data collection time is roughly 10 minutes. The sonographer collects tracked B-mode, strain, and RF data as described in Section 2.1. We use Siemens eSie Touch Elasticity imaging for real-time feedback to the user. For off-line processing, an algorithm based on dynamic programming (DP) introduced in[13] calculates high quality strain images from RF data.

The preliminary results of our experiments show the potential of our proposed methodology in resolving ambiguities for delineation of lumpectomy cavity. Figure 5(a) demonstrates one cross-section of the CT volume resliced based on the origin and orientation of B-mode image shown in Figure 5(c). The white rectangle in Figure 5(a) is magnified and presented in Figure 5(b). This image corresponds to the same B-mode image of Figure 5(c).

The poor local resolution of CT scan challenges accurate segmentation of the boundary of the cavity, whereas fine details are detectable in the ultrasound image.

The depth and pixel size of the images were 6 cm and 0.17 mm respectively. The data capture speed ranged from 10 to 30 frames per second selected by user depending on the ultrasound frame rate and the speed of freehand scanning. The CT volumes had a pixel size of about 1.2 mm and slice thickness of 3 mm.

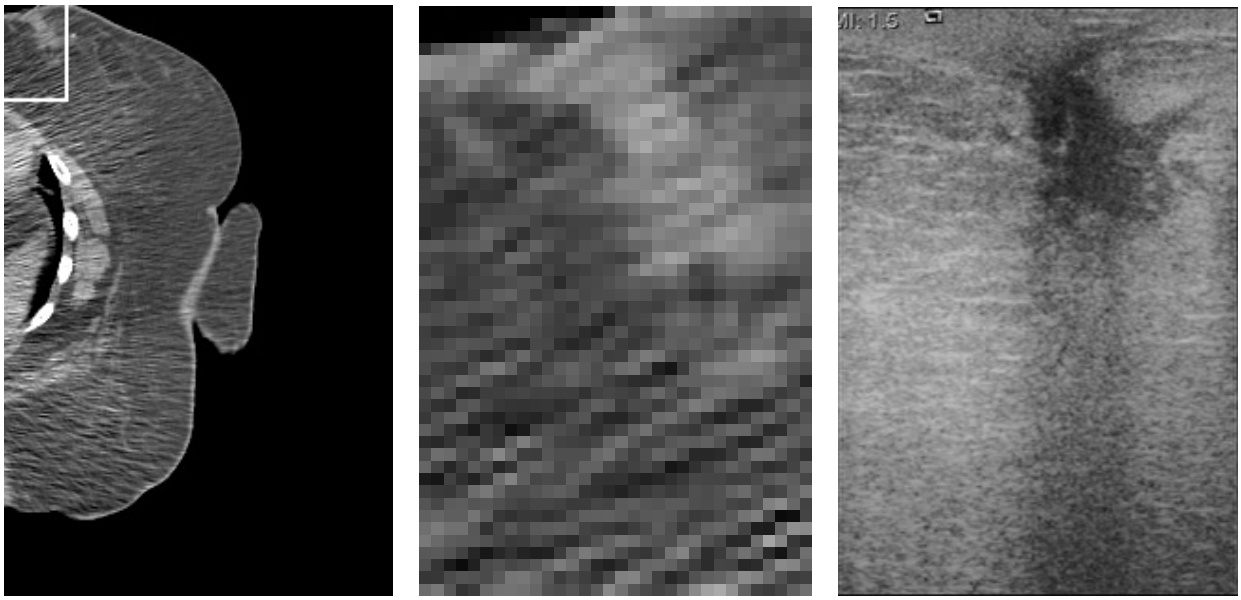

(a) Resliced CT (b) Magnified CT (c) B-mode image

Figure 5. Comparison of CT and ultrasound cross sections. a) shows the cross-section of CT volume resliced based on B-mode image in c). b) depicts the white rectangle in a) and corresponds to c). The figures show superior resolution of ultrasound revealing structural details that are not visible in CT.

4. CONCLUSION AND FUTURE WORK

PBI cannot succeed without precise and accurate lumpectomy cavity localization, a problem that has no solution today. Our proposed visualization prototype system has the potential to help precise cavity delineation and targeting. The system introduces minimal deviation from the standard workflow of EBRT procedure. little additional time is required for acquisition of the 3D-US and strain images. The delineation is still performed on readily available clinical computer stations while 3D-US and strain images offers additional information to resolve ambiguities in delineating the lumpectomy bed. The successful deployment of this system should enable accurate targeting for PBI. Moreover, monitoring stiffness during the treatment course might disclose important clinical information which may impact the process of treatment.

The adaptive selection of RF data based on tracking can facilitate the wide use of strain imaging by reducing the dependency of the quality of the images on users' expertise. Inclusion of tracking information in strain calculation has shown a great potential. In order to further develop this technique and merge it into our system, we are investigating the tools needed for real-time and direct access to RF data. At the same time, we are working on fast and robust strain imaging techniques for real-time feedback as the user collects the data.

A long-term investigation is necessary for a concrete conclusion about the overall effectiveness of the proposed planning system on PBI treatment. In this paper, we illustrated our new planing scheme for PBI, the system developed to realize it, and the experiments for initial assessment. The following step includes a thorough multiuser evaluation of the accuracy of delineation with and without our planning system. This study shows whether the system reduces uncertainty in delineation among users and over time. The ultimate goal would be to determine the impact of precise delineation on reducing the treatment side-effects and preventing the recurrence of cancer.

5. ACKNOWLEDGMENT

The authors would like to thank Siemens Corp. for loaning the US machine and Shelby Brunke for his support and help with the US machine. This work is supported in part by Breast Cancer Research Foundation (BCRF).

REFERENCES

[1] Baglan, K. L. and et. al, "Accelerated partial breast irradiation using 3d conformal radiation therapy 3D-CRT," *Int. J. Radiat. Oncol. Biol. Phys.* **55**(2), 302–311 (2003).

[2] Benda, R. K., Yasuda, G., Sethi, A., Gabram, S. G., Hinerman, R. W., and Mendenhall, N. P., "Breast boost: are we missing the target?," *Cancer* **97**(4), 905–909 (2003).

[3] Fitzpatrick, J. M. and West, J. B., "The distribution of target registration error in rigid-body point-based registration," *IEEE Transactions on Medical Imaging* **20**(9), 917–927 (2001).

[4] Letourneau, D. and et. al, "Cone-beam-CT guided radiation therapy: technical implementation," *Radiother. Oncol.* **75**(3), 279–286 (2005).

[5] Nikolaou, K., Flohr, T., Stierstorfer, K., Becker, C. R., and Reiser, M. F., "Flat panel computed tomography of human ex vivo heart and bone specimens: initial experience," *Eur. Radiol.* **15**(2), 329–333 (2005).

[6] Vences, L., Wulf, J., Vordermark, D., Sauer, O., Berlinger, K., and Roth, M., "Target motion measurement without implanted markers and its validation by comparison with manually obtained data," *Med. Phys.* **32**(11), 3431–3439 (2005).

[7] Jaffray, D. A., Siewerdsen, J. H., Wong, J. W., and Martinez, A. A., "Flat-panel cone-beam computed tomography for image-guided radiation therapy," *Int. J. Radiat. Oncol. Biol. Phys.* **53**(5), 1337–1349 (2002).

[8] Landis, D. M. and et. al, "Variability among breast radiation oncologists in delineation of the postsurgical lumpectomy cavity," *Int. J. Radiat. Oncol. Biol. Phys.* **67**(5), 1299–1308 (2007).

[9] Hurkmans, C., Admiraal, M., van der Sangen, M., and Dijkmans, I., "Significance of breast boost volume changes during radiotherapy in relation to current clinical interobserver variations," *Radiother. Oncol.* (2008).

[10] Langen, K. M. and et. al, "Evaluation of ultrasound-based prostate localization for image-guided radiotherapy," *Int. J. Radiat. Oncol. Biol. Phys.* **57**(3), 635–644 (2003).

[11] Chandra, A. and et. al, "Experience of ultrasound-based daily prostate localization," *Int. J. Radiat. Oncol. Biol. Phys.* **56**(2), 436–447 (2003).

[12] Prager, R. W., Rohling, R. N., Gee, A. H., and Berman, L., "Rapid calibration for 3-D freehand ultrasound," *Ultrasound in Medicine and Biology* **24**(6), 855–869 (1998).

[13] Rivaz, H., Boctor, E., Foroughi, P., Zellars, R., Fichtinger, G., and Hager, G., "Ultrasound elastography: a dynamic programming approach," *IEEE Transaction in Medical Imaging* **27**, 1373–1377 (October 2008).

[14] Shoemake, K., "Animating rotation with quaternion curves," *Computer Graphics (Proc. of SIGGRAPH)* , 245–254 (1985).